SECURITY CLASSIFICATION OF THIS PAGE (When Data Entered)

REPORT DOCUMENTATION PAGE		READ INSTRUCTIONS BEFORE COMPLETING FORM
1. REPORT NUMBER NRL Memorandum Report 5011	2. GOVT ACCESSION NO. AD-A126306	3. RECIPIENT'S CATALOG NUMBER
4. TITLE (and Subtitle) START-UP OF A PULSED BEAM FREE ELECTRON LASER (FEL) OSCILLATOR		5. TYPE OF REPORT & PERIOD COVERED Interim report on a continuing NRL problem. 6. PERFORMING ORG. REPORT NUMBER
7. AUTHOR(s) P. Sprangle, C.M. Tang and Ira B. Bernstein*		8. CONTRACT OR GRANT NUMBER(s)
9. PERFORMING ORGANIZATION NAME AND ADDRESS Naval Research Laboratory Washington, D.C. 20375		10. PROGRAM ELEMENT, PROJECT, TASK AREA & WORK UNIT NUMBERS 62301E; 47-0867-0-2
11. CONTROLLING OFFICE NAME AND ADDRESS Defense Advanced Research Projects Agency Arlington, VA 22209		12. REPORT DATE April 1, 1983 13. NUMBER OF PAGES 15
14. MONITORING AGENCY NAME & ADDRESS(if different from Controlling Office)		15. SECURITY CLASS. (of this report) UNCLASSIFIED 15a. DECLASSIFICATION/DOWNGRADING SCHEDULE

16. DISTRIBUTION STATEMENT (of this Report)

Approved for public release; distribution unlimited.

17. DISTRIBUTION STATEMENT (of the abstract entered in Block 20, if different from Report)

18. SUPPLEMENTARY NOTES

*Present address: Yale University, New Haven, CT

This work was supported by DARPA under contract No. 3817.

19. KEY WORDS (Continue on reverse side if necessary and identify by block number)

Free electron laser Oscillator Start-up

20. ABSTRACT (Continue on reverse side if necessary and identify by block number)

A one-dimensional linear analysis is presented of the start-up of an FEL oscillator. The model treats electron beam pulses of arbitrary shape and many significant three dimensional effects are included heuristically. A closed equation is derived for the ensemble averaged electromagnetic energy density matrix which contains the spontaneous emission as a source, and which represents the small gain per pass and losses via coefficient matrices. Numerical solutions are compared with the Stanford experimental results.

DD FORM 1 JAN 73 1473 EDITION OF 1 NOV 65 IS OBSOLETE
S/N 0102-014-6601

SECURITY CLASSIFICATION OF THIS PAGE (When Data Entered)

START-UP OF A PULSED BEAM FREE ELECTRON LASER (FEL) OSCILLATOR

A number of successful free electron laser oscillator experiments have been reported.[1-4] Simple considerations concerning the spontaneous radiation level indicated start-up times much shorter than those observed.[3,4] Therefore, since a number of experiments utilizing shorter electron beam macropulses are being constructed or planned, there is concern that these forthcoming experiments may not be able to achieve saturation. A quantitative understanding of the basic process governing the growth of coherent stimulated radiation from incoherent spontaneous emission is therefore highly desirable. This is especially true since the device is very sensitive to small changes in parameters. A quantitative understanding of the coherent gain is available, but the analysis of the coupling to the incoherent emission is incomplete. Here we outline a classical one-dimensional theory of the start-up of the FEL oscillator in the cold, small signal regime. Certain important three dimensional effects are incorporated heuristically by means of filling factors. The statistical features of the problem lead to a formulation in terms of an ensemble averaged energy density matrix $\underline{\underline{\varepsilon}}$, a diagonal element of which is proportional to the fraction of the electromagnetic field energy in the associated Fourier component. This matrix obeys a linear equation in which the inhomogeneous term represents the ensemble average emission, and gain and loss appear in coefficient matrices. The non-diagonal terms of $\underline{\underline{\varepsilon}}$ yield information on the cross correlations between Fourier components.

Theories of the FEL[5-9] proceed from a continuum description of the electron dynamics, either fluid equations or the Vlasov equation. A proper description of the start-up of an FEL oscillator, however, must take into account the fact the electrons are discrete and substantially uncorrelated, since it is the acceleration radiation of individual electrons in the wiggler

Manuscript approved January 10, 1983.

that provides the initial fields. The acceleration radiation is then amplified by the collective gain mechanism associated with the continuum description. Thus a statistical theory is required, couched in terms of objects bilinear in the fluctuating quantities so that ensemble averages are non-zero, even when the ensemble averages of the fluctuating current density vanish.

The theory developed here is one-dimensional in space and treats the electrons as governed by Maxwell's equations. The wiggler is approximated by the vector potential $\underset{\sim}{A}_w = A_w \cos(k_w z)\, \theta(z - L_o)\, \theta(L_o + L_w - z)\, \hat{e}_x$ where $\theta(x)$ is the step function and A_w and $k_w = 2\pi/\ell_w$ are constants. The radiation vector potential is written as $\underset{\sim}{A}_R(z,t) = \sum_{n=1}^{\infty} a_n(t) \sin k_n z \exp(i\omega_n t)\, \hat{e}_x + \text{c.c.}$, where $k_n = \omega_n/c = n\pi/L$, the separation between the mirrors is L (see Fig 1), $a_n(t)$ is taken to be slowly varying in time, and the tangential component of the electric field $\underset{\sim}{E} = -c^{-1}\partial \underset{\sim}{A}_R/\partial t$ vanishes on the mirrors. In what follows we will assume that $|\underset{\sim}{A}_w| \gg |\underset{\sim}{A}_R|$. The current density driving $\underset{\sim}{A}_R$ can be written as $\underset{\sim}{J}(z,t) = \underset{\sim}{J}_c(z,t) + \underset{\sim}{J}_{inc}(z,t)$ where $\underset{\sim}{J}_c$ is the coherent current driving the stimulated radiation (gain) and $\underset{\sim}{J}_{inc}$ is the incoherent current due to the discrete nature of the electrons and is responsible for the spontaneous radiation (shot noise). The coherent and incoherent current densities are respectively given by $\underset{\sim}{J}_c = -|e|\underset{\sim}{v}_w F_c \langle n(z,t)\rangle$ and $\underset{\sim}{J}_{inc} = -|e|\underset{\sim}{v}_w F_{inc}[n(z,t) - \langle n(z,t)\rangle]$ where $\underset{\sim}{v}_w = c\underset{\sim}{\beta}_w = |e|\underset{\sim}{A}_w(z)/\gamma_o m_o c$ is the wiggler velocity. The actual discrete electron density is $n(z,t) = \sigma_b^{-1} \sum_j \delta(z - \tilde{z}_j(t))$ where σ_b is the transverse electron beam area and the lateral distribution of electrons has been treated as uniform. Only axial discreteness is included. The ensemble average over the initially uncorrelated electrons is denoted by $\langle\ \rangle$, hence $\langle n(z,t)\rangle$ is the continuum

electron density and $n(z,t) - \langle n(z,t)\rangle$ represents the fluctuating part of the density. The usual filling factor is $F_c = \sigma_b/\sigma_r$, where σ_r is the transverse area of the resonator radiation mode; F_{inc} is the filling factor associated with the incoherent radiation and is somewhat more involved. It can be shown that $F_{inc} = \sigma_b(\lambda_L\gamma)^{-2} f_m$ where $\lambda_L = \ell_w(1 + v_{oz}/c)^{-1}\gamma_{oz}^{-2}$ is the characteristic laser wavelength and f_m is a loss factor due to the finite size of the mirror located at $z = L$. The loss factor for the incoherent radiation is $f_m \approx [2\gamma r_m/(1 + \gamma\beta_w)L]^2$ where r_m is the mirror radius. In computing f_m we have taken the incoherent radiation divergence angle to be $\approx (1/\gamma + \beta_w)$.

The equation of motion for the jth electron is

$\ddot{\tilde{z}}_j = -(|e|/\gamma_o m_o c)^2(\partial/\partial z - c^{-2}v_{oz}\partial/\partial t)(\underset{\sim}{A}_w(z) \cdot \underset{\sim}{A}_R(z,t))\,|_{z = \tilde{z}_j}$ where the right hand side is the ponderomotive acceleration. The initial conditions are $\tilde{z}_j(t_j) = 0$, and $\dot{\tilde{z}}_j(t_j) = v_{oz}$.

The radiation vector potential obeys

$(\partial^2/\partial z^2 - c^{-2}\partial^2/\partial t^2 - c^{-2}\nu\partial/\partial t)\underset{\sim}{A}_R = -4\pi c^{-1}\underset{\sim}{J}$, where $\nu = \omega_L/Q$, $\omega_L = 2\pi c/\lambda_L$ is the characteristic upshifted frequency, $v_{oz} = c\beta_{oz}$ is the unperturbed axial pulse velocity, and Q is the quality factor of the resonator.

These equations when linearized yield a set of coupled linear equations, the homogeneous part of which describes the coherent phenomena, and the inhomogeneous part (involving the fluctuation in the electron density) represents the incoherent emission. The incoherent (spontaneous) emission part of a_n satisfies $\langle a_n\rangle = 0$. Thus in order to obtain non-trivial statistical information one defines the total radiation energy density matrix $\varepsilon_{nm}(t) = k_n k_m \langle a_n(t)\, a_m^*(t)\rangle$. Note that $\varepsilon_{nn} = k_n^2\langle|a_n|^2\rangle$ is proportional to the ensemble average energy density in the nth Fourier component, and ε_{nm} is related to the correlation of the nth and mth Fourier components of the

electric field. These statistical quantities are measurable. It may be shown after considerable calculation that when the gain per pass is small

$$\underline{\underline{\varepsilon}}(t_N+\tau) = (1-\frac{\nu}{c^2})\,\underline{\underline{\varepsilon}}(t_N) + \underline{\underline{G}}\,(t_N,\tau)\cdot\underline{\underline{\varepsilon}}(t_N) + \underline{\underline{\varepsilon}}(t_N)\cdot\underline{\underline{G}}^H(t_N,\tau) + \underline{\underline{S}}(t_N,\tau) \tag{1}$$

where the matrix $\underline{\underline{G}}$ enbodies the coherent response, $\underline{\underline{S}}$ represents the spontaneous emission, t_N is the time the Nth electron pulse entered the wiggler and H denotes the Hermitian conjugate. Indeed the trace of $\underline{\underline{S}}$ is proportional to the total spontaneous energy radiated by one pulse of electrons in traversing the wiggler. The elements of the gain matrix and the source matrix at time $t_N + \tau$ are given by

$$G_{nm}(t_N+\tau) = \frac{-i}{32}\frac{\ell_b}{L}\,\frac{\omega_b^2}{\gamma_o}\,\frac{v_w^2}{c^2}\,k_w c\,F_c e^{2i\pi(n-m)(N-1)\,\delta L/L}\,\alpha_{nm}\rho_{nm}g_{nm}(\tau),$$

$$S_{nm}(t_N+\tau) = \frac{\ell_b}{2L}\,\frac{\pi^2|e|^2 n_o v_w^2 F_{inc}}{L\sigma_b}\,e^{2i\pi(n-m)(N-1)\delta L/L}\,\alpha_{nm}\,\rho_{nm}\,h_{nm}(\tau)$$

where

$$g_{nm}(\tau) = \frac{\tau^3}{x_n x_m^2}\left(e^{ix_n}(1+\frac{x_m}{x_n})\,\sin x_n - e^{i(x_n-x_m)}\,x_n\,\left(\frac{\sin(x_n-x_m)}{x_n-x_m}\right) - x_m e^{2ix_n}\right),$$

$$h_{nm}(\tau) = \frac{\tau^2}{x_n x_m}\{(\sin^2 x_n + \sin^2 x_m - \sin^2(x_n-x_m))$$

$$- i(\sin x_n\cos x_n - \sin x_m\cos x_m - \sin(x_n-x_m)\cos(x_n-x_m))\},$$

$$\alpha_{nm} = \exp(-i(k_n - k_m)(1-\beta_o)\beta_o^{-1}L_o), \quad x_n = [v_{oz}k_w - ck_n(1 - v_{oz}/c)]\tau/2,$$

$$\rho_{nm} = \begin{cases} \frac{\sqrt{\pi}}{2} e^{-((k_n - k_m)\ell_b/4)^2}, & \text{for Gaussian electron pulse profile} \\ \frac{\sin(k_n - k_m)\ell_b/2}{(k_n - k_m)\ell_b/2}, & \text{for square shaped electron pulse profile,} \end{cases}$$

$\beta_o = v_o/c$, $\omega_b^2 = 4\pi|e|^2 n_o/m_o$ and $\delta L = L - L_b/2\beta_o$. The matrices $\underline{\underline{\varepsilon}}$ and $\underline{\underline{S}}$ are Hermitian.

Equation (1) has been integrated numerically to obtain $\underline{\underline{\varepsilon}}$. The parameters employed in the numerical studies are given in Table 1, corresponding to the Stanford experiment.[4] Figure 2 shows the peak radiation power within the resonator as a function of the number of beam pulses that have traversed the resonator for various values of resonator length mismatch $\delta L = L - L_b/2\beta_o$. Figure 3 shows the asymptotic gain as a function of δL. The mirror mismatch $\delta L = -1.1 \times 10^{-3}$ cm corresponds to maximum gain but not maximum saturated power. Maximum saturated power occurs for δL between 0 and -1.1×10^{-3} cm. The range in δL for nonzero gain is -3.0×10^{-3} cm$< \delta L < 0$, in fair agreement with the experimental range of 2.5×10^{-3} cm. The maximum calculated multi-mode (finite beam pulse) energy gain is 0.16 whereas the single mode (continuous beam) yields a value of 0.25. Finite beam pulse effects therefore reduce the linear gain by approximately 60%. The maximum observed gain is 0.10.

Figure 4 shows the spatial distribution of the electron pulses (square) and the radiation power pulse at the entrance and exit of the wiggler for $\delta L = -1.0 \times 10^{-3}$ cm. Upon entering the wiggler the radiation pulse slightly lags the beam pulse, while at the exit of the wiggler the two are completely overlapped. Figure 5 shows the energy spectrum of the radiation

pulse after 100 beam pulses. The spontaneous radiation energy spectrum is also shown for reference purposes.

Equation (4) suggests that one can roughly compute the relationship between P_N, the peak power in the resonator after the Nth pulse, to P_o, the power emitted spontaneously, by assuming a constant average gain per pass g. An elementary calculation yields when $N \gg 1$ and $g \ll 1$, $P_N/P_o = N - 1 + (1 + g)^N \approx N + \exp(gN)$. Clearly when $gN \gg 1$ the result is very sensitive to small changes in g and N. If one takes the experimental values corresponding to the maximum observed final power of $P_N = 2.7 \times 10^7$ W within the resonator, $N = 540$ and the computed spontaneous power of $P_o = 6.5 \times 10^{-2}$ W, one finds that $g = 0.037$. The experimental value of the linear gain is 0.067. In view of the sensitivity to changes in N and g the results are not inconsistent. Moreover this effective value of g is smaller than the linear gain predicted by the present model which is reasonable since non-linear effects and initial beam thermal effects must lower the gain. Unfortunately the currently available data is inadequate to make other detailed comparisons with this small-signal theory.

Our analysis immediately suggest possible ways to substantially shorten the oscillator start-up time while maintaining high saturated power levels. The first approach takes advantage of the fact that the maximum linear gain and maximum saturated power occur for different values of δL, which we will respectively denote by δL_1 and δL_2. By slightly increasing the frequency of the R.F. accelerating field, ω_{acc}, during the start-up period, i.e., decreasing the beam pulse separation, the value of δL, could be varied from an initial value of δL_1 to the value of δL_2, thus, decreasing the start-up time while maintaining high final power levels. The required fractional increase in ω_{acc} is $|\delta L_1 - \delta L_2|/L_b \approx 10^{-6}$ for the parameters of ref. (3,4). The same

effect may also be realized by simply changing (increasing) the mirror separation during the start-up period. Another possible method of decreasing the start-up time would be to simply increase that part of F_{inc} associated with mirror losses, i.e., increase f_m. This could be accomplished by increasing the effective size of the mirror located at z = L. The additional extension of the mirror would necessarily have a different curvature. This last approach should make it possible to contain a far larger portion of the incoherent radiation.

Acknowledgment

The authors are grateful to Dr. W. Colson for many illuminating discussions. This work was supported by DARPA under contract No. 3817.

Table I

Beam Parameters

Beam Energy, $(\gamma_o - 1)m_o c^2$	43 MeV
Total Gamma, γ_o	85
Axial Gamma, γ_{oz}	69
Peak Current, I_p	1.3 A
Pulse Width, ℓ_b	0.75 mm
Pulse Separation, L_b	25.4 m
Beam Radius, r_b	0.25 mm

Wiggler Parameters

Wavelength, ℓ_w	3.3 cm
Amplitude (helical), B_w	2.3 kG
Length, L_w	5.3 m

Resonator and Radiation

Resonator Length, L	12.7 m
Resonator Losses (round trip)	1.5%
Radiation Wavelength, λ_L	3.3 μm
Spot Size, r_o	0.167 cm
Beam Filling Factor, F_c	0.017
Incoh. Rad. Loss Factor, f_m	0.05

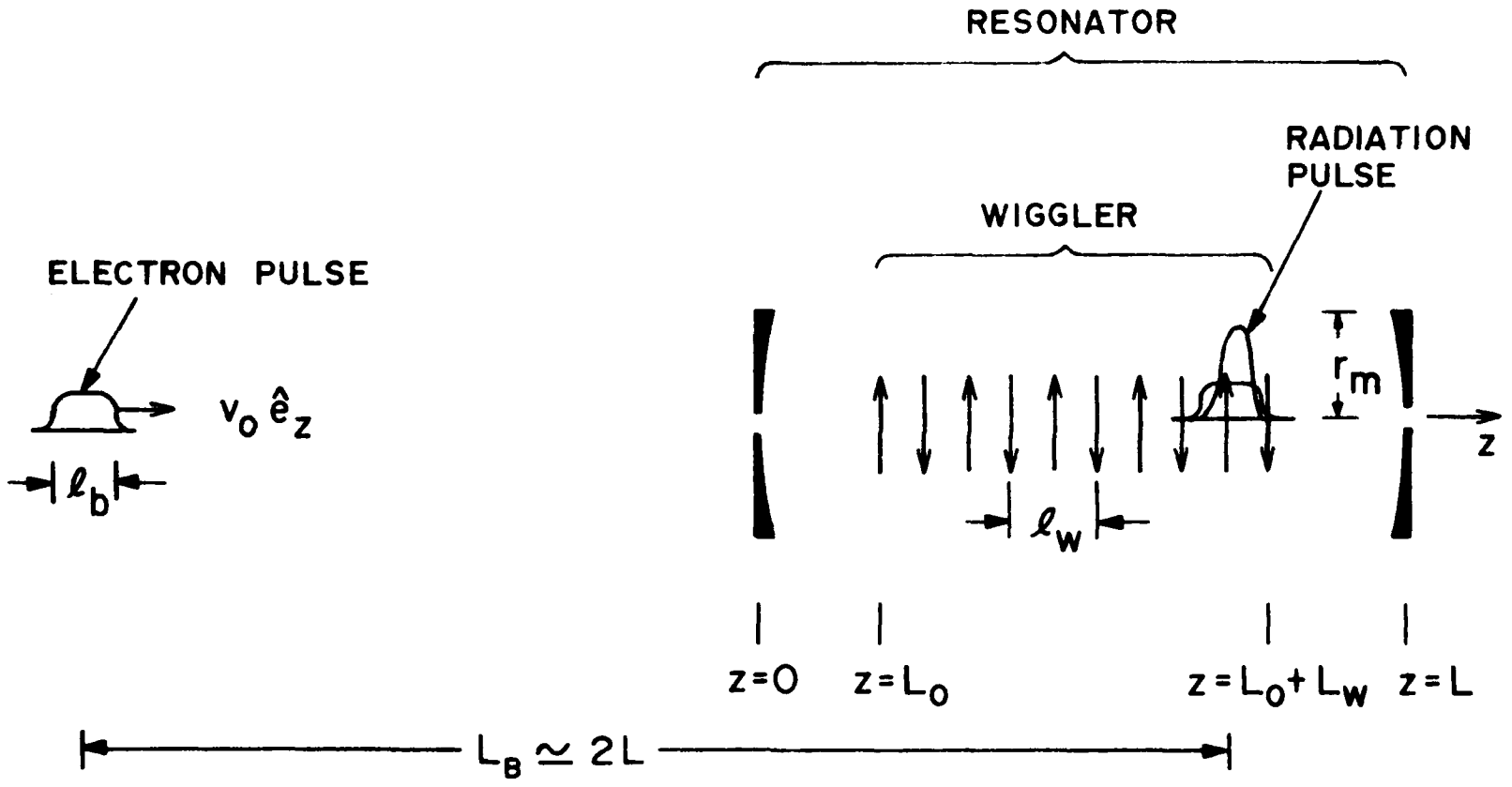

Fig. 1 Schematic of a pulsed electron beam FEL oscillator.

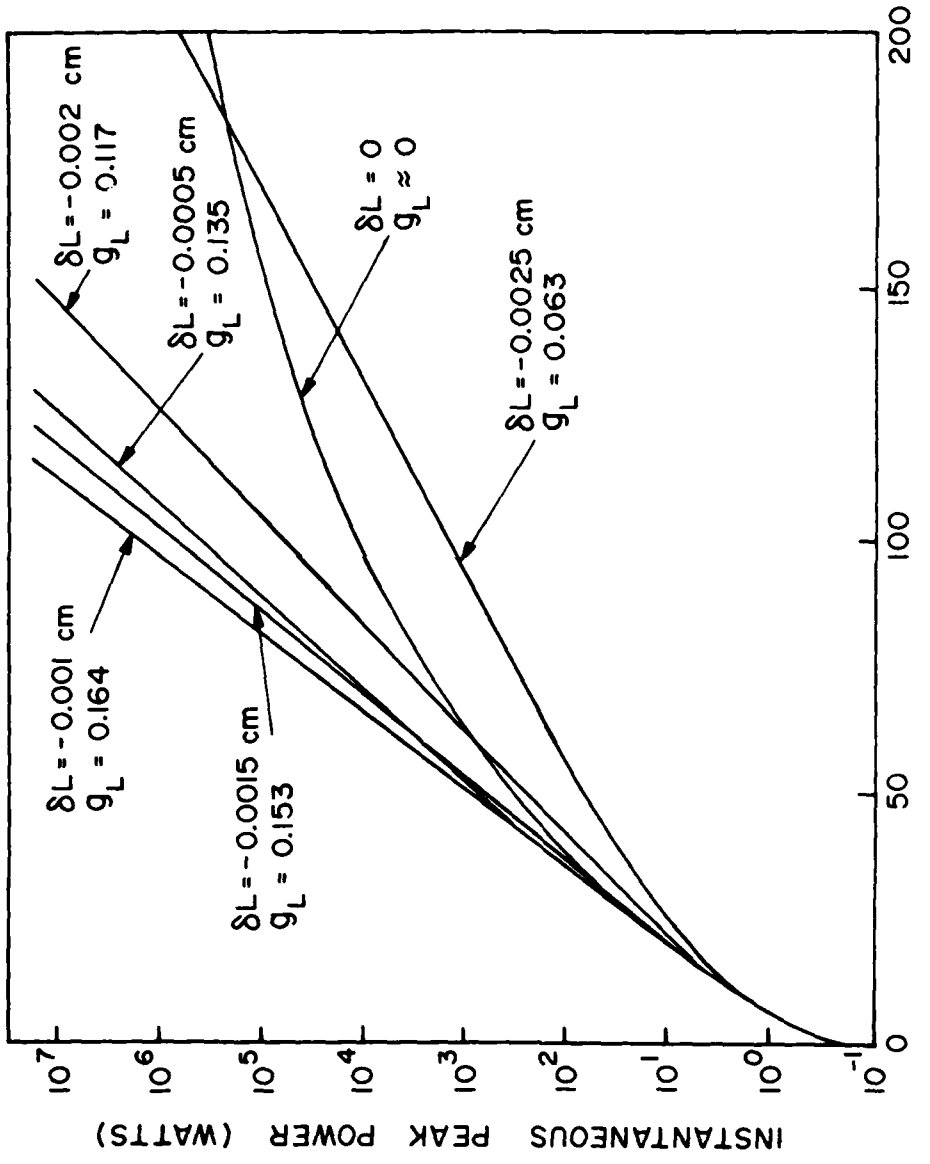

Fig. 2 Peak power of the radiation pulse as a function of the number of passes for various detuning parameters δL.

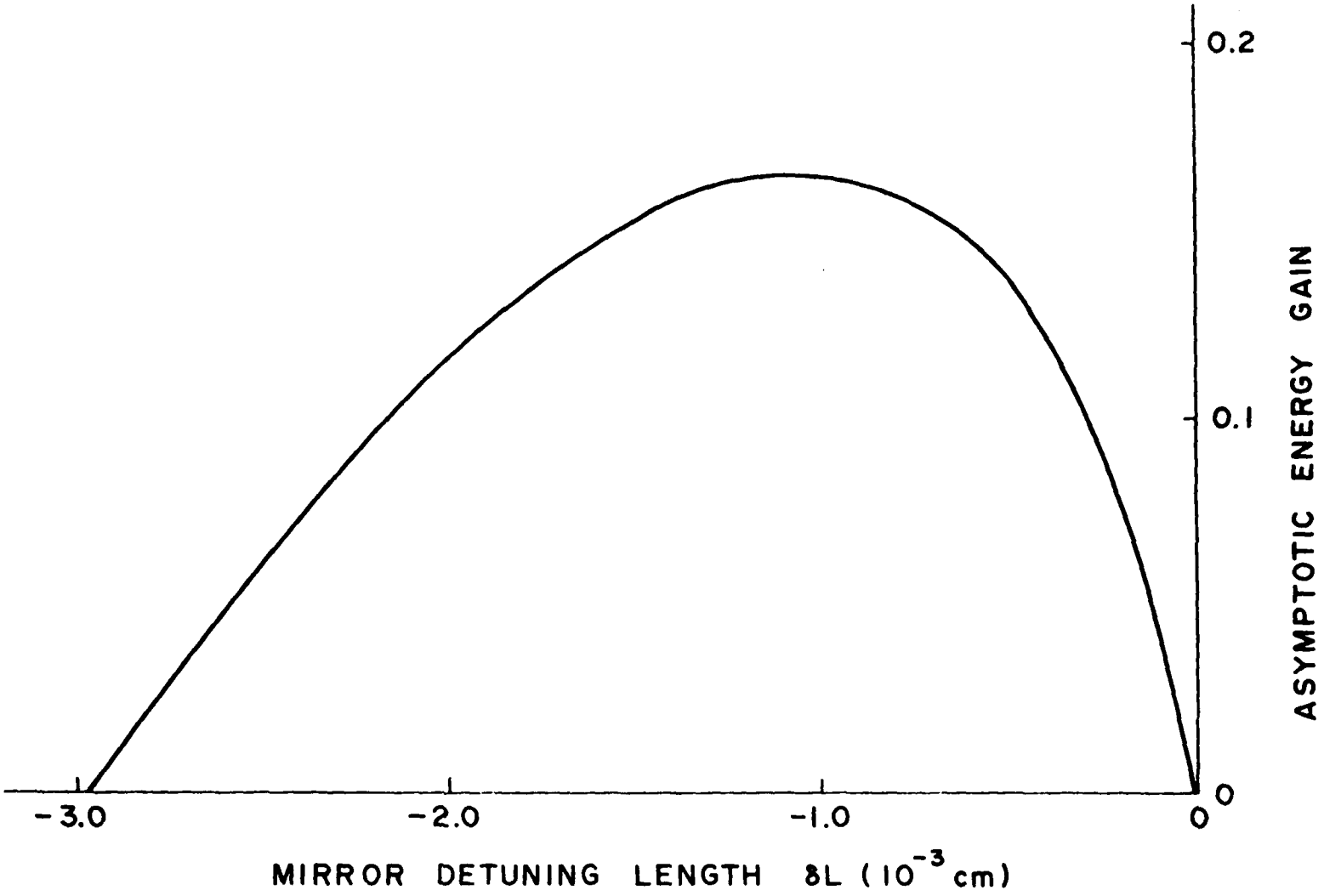

Fig. 3 Asymptotic energy gain ($t_N >> 2L/v_{zo}$) of the radiation pulse as a function of δL.

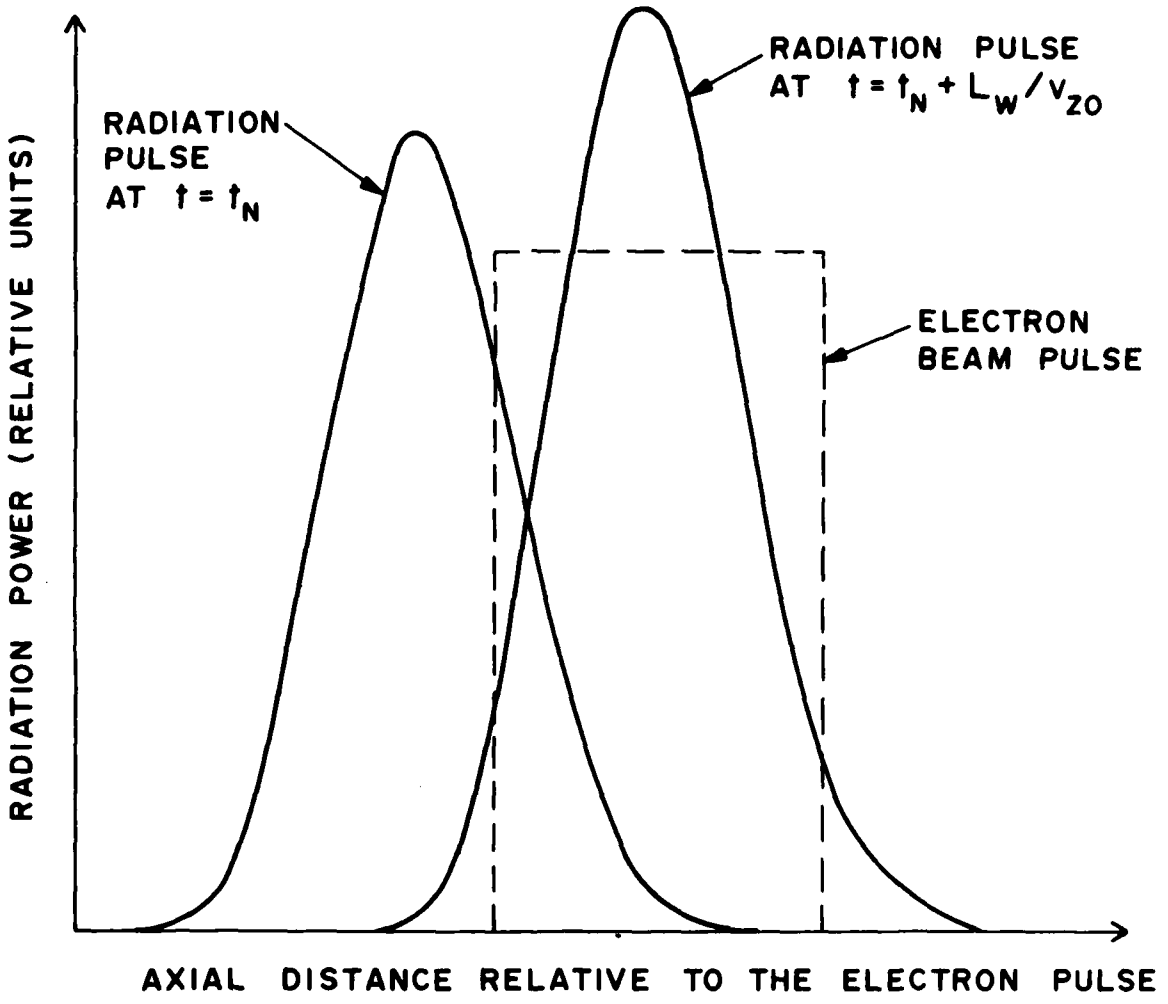

Fig. 4 Radiation pulse power relative to the spatial distribution of the electron pulse (square) at the entrance of the wiggler ($t = t_N$) and exit of wiggler ($t = t_N + L_w/v_{zo}$), where $N >> 1$ denotes the electron pulse number.

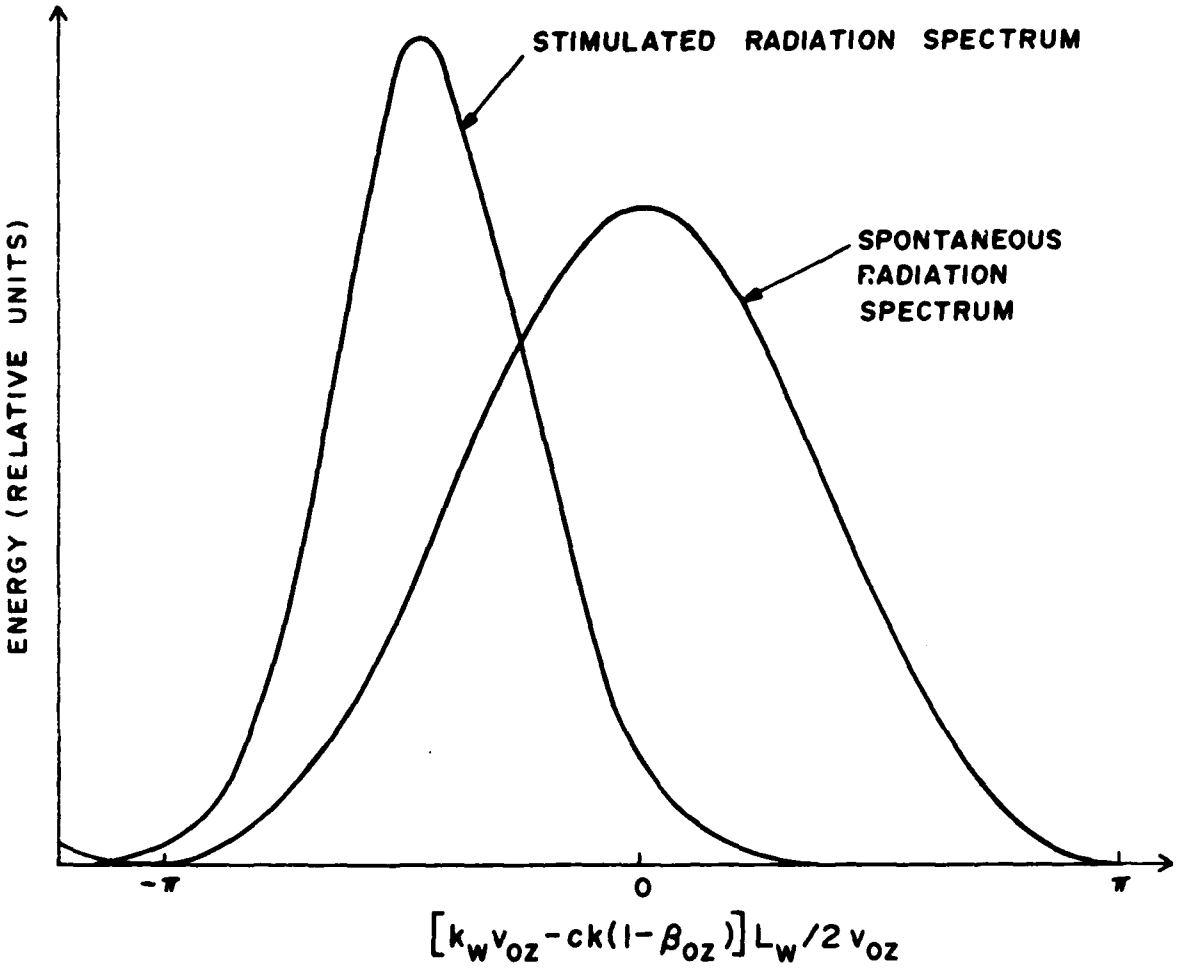

Fig. 5 Asymptotic energy spectrum of the radiation pulse.

References

1. D. A. G. Deacon, et al., Phys. Rev. Lett. 38, 892 (1977).
2. J. M. J. Madey, et al., Final Technical Report to ERDA, Contracts FY-76-03-0326 PA 48 and PA 49 (1977).
3. J. N. Eckstein, et al., Physics of Quantum Electronics, Chap. 2, Vol 8, ed. Jacobs, Pilloff, Scully, Moore, Sargent and Spitzer, Addison-Wesley, Reading MA, 49 (1982).
4. S. Benson, et al., to be published in the proceedings of Bendor Free Electron Laser Conference, Bendor, France, Sep 27-Oct 1, 1982.
5. P. Sprangle, C.-M. Tang and W. M. Manheimer, Phys. Rev. A21, 302 (1980).
6. N. M. Kroll, P. L. Morton and M. N. Rosenbluth, IEEE J. of Quantum Electronics, QE-17, 1436 (1981).
7. G. Dattoli, A. Marino, A. Renieri, and F. Romanelli, IEEE J. of Quantum Electronics, QE-17, 1371 (1981).
8. P. Sprangle and C.-M. Tang, Appl. Phys. Lett. 39, 677 (1981) and C.-M. Tang and P. Sprangle, Chap. 27, Vol 9, Ref. 3, 627 (1982).
9. W. B. Colson, Chap. 19, Vol 8, Ref. 3, 457 (1982).